

Spatial variation in the ^{137}Cs inventory in soils in a mixed deciduous forest in Fukushima, Japan



Momo Takada ^{a,*}, Toshihiro Yamada ^a, Teruhiko Takahara ^{a,b}, Toshinori Okuda ^a

^a Graduate School of Integrated Arts and Sciences, Hiroshima University, 1-7-1 Kagamiyama, Higashi-Hiroshima, 739-8521, Japan

^b Faculty of Life and Environmental Science, Shimane University, 1060 Nishikawatsu, Matsue, Shimane, 690-8504, Japan

ARTICLE INFO

Article history:

Received 11 March 2016

Received in revised form

22 April 2016

Accepted 25 April 2016

Available online 9 May 2016

Keywords:

Spatial heterogeneity

Radiocesium

Stemflow

Throughfall

Canopy interception

ABSTRACT

The spatial variation of the radiocesium inventory in forest soil was studied c.a. 44 km northwest of the Fukushima Daiichi Nuclear Power Plant, Japan. This study focuses on the effects of canopy interception and downward transfer from the forest canopy to the forest floor via stemflow and throughfall. We established a study plot (400 m²) in the canopy layer of a secondary mixed deciduous forest dominated by Japanese oak (*Quercus crispula*) and Japanese fir (*Abies firma*), in August and November 2014. Soil was sampled from 0 to 5 cm depth and ^{137}Cs was measured under the canopy using a 2-m grid and also at the tree trunk bases. We divided the study plot into the five different types of subplot according to the canopy projection areas and the tree species for the analysis. The geometric mean and coefficient of variation of the ^{137}Cs inventory were 202 kBq m⁻² and 0.11 (0.52 in the arithmetic coefficient of variation), respectively. Within the forest, the variation in the ^{137}Cs inventory under trees was larger than in crown gap areas. The large spatial variation may be attributed to canopy interception of the initial deposition and downward transfer of radiocesium via stemflow and throughfall.

© 2016 Elsevier Ltd. All rights reserved.

1. Introduction

The Fukushima Daiichi Nuclear Power Plant (FDNPP) accident in Japan in 2011 released various types of radionuclide into the environment (Endo et al., 2012; Yoshida and Kanda, 2012). More than 70% of the contaminated areas in Fukushima and the neighboring prefectures are forests, and a large amount of radiocesium (specifically, ^{137}Cs) will remain in these areas for a considerable time because of its long half-life of 30.17 years (Kuroda et al., 2013; Loffredo et al., 2014). Studies into the dynamics of radiocesium within a forest ecosystem will be important over the coming decades in applications such as forest management and radiation protection when resuming the use of the forest resources (Hashimoto et al., 2013; Fujii et al., 2014).

According to previous studies, radiocesium released into the atmosphere after the FDNPP accident was initially deposited not only on forest floors but also intercepted by tree bodies (tree crowns, branches, and stems; Hashimoto et al., 2013; Kato et al., 2015). At the time of the FDNPP accident in Fukushima Prefecture, canopy interception was expected to be approximately 70%

and 20% of the total deposition in evergreen and deciduous forests, respectively (Kato et al., 2015). Canopy interception of radiocesium derived from the Chernobyl nuclear power plant accident is reported to account for 70% of the total deposition, and the radiocesium remains on canopies for several years (Bunzl et al., 1989). The radiocesium intercepted by the tree bodies is transferred onto the forest floor via stemflow, throughfall by precipitation, and directly from litterfall (Rafferty et al., 2000). Most of the radiocesium on the tree canopies was transferred on to forest floors and soils through these processes in the Fukushima region (Hisadome et al., 2013; Endo et al., 2015; Kato et al., 2012). Radiocesium within the litter on the forest floor is released into the forest soil following litter decomposition (Rafferty et al., 1997, 2000), and the decomposition process in the Fukushima region is completed within several years (Ono et al., 2013). As a result, most of the radiocesium present within the forest several years after the FDNPP accident is now present in soil (Hashimoto et al., 2013), and is expected to remain in the soil for a long time as radiocesium adsorbed on soil particles has a low mobility (Schimmack et al., 1994; Matsunaga et al., 2013). Therefore, studies on the radiocesium dynamics in forest soils are important when considering forest management and radiation protection for resuming the use of the forest resources.

* Corresponding author. Tel.: +81 82 424 6513; fax: +81 84 424 0758.

E-mail address: taka-momo@hiroshima-u.ac.jp (M. Takada).

In a forest ecosystem, the spatial heterogeneity of the soil radiocesium inventory represents a major difficulty for studying the dynamics. This limitation has been discussed for some years and various studies have been conducted that aim toward a more accurate and precise evaluation (Guillitte et al., 1990; Khomutin et al., 2004; Korobova and Romanov, 2009, 2011). However, to our knowledge, no studies have examined the characteristics of the spatial heterogeneity by comparing with other ecosystems such as open areas, grasslands and croplands. As described above, spatial distribution of radiocesium in the forest soils of Fukushima Prefecture three years after the FDNPP accident is expected to be affected by canopy interception of initial deposition and translocation from the canopy to the forest floor via throughfall, stemflow and litterfall. Consequently, the spatial distribution in forest soil may differ with those in other ecosystems.

Therefore, in the present study, we conducted field surveys in a mixed deciduous forest in Fukushima to evaluate the spatial variation of the soil radiocesium inventory. To clarify effects of canopy interception, precipitation (throughfall and stemflow) and litterfall, we divided the study plot into five subplot types according to canopy projection areas and the tree species, and then examined the spatial variation of radiocesium inventory in each of these subplot types.

2. Materials and methods

2.1. Study site

The study site is a secondary mixed deciduous forest, located in Soma in the northern part of Japan, 44 km northwest of the FDNPP (37°45' N, 140°47' E; 570 m asl, Fig. 1). The study site was positioned in a flat area on a mountainside, and the surrounding environment was same as the study plot. At the time of the FDNPP accident, the radioactive plume was estimated to arrive at the present study site from the southeast side (Katata et al., 2012), and the ratio of wet deposition to the total ^{137}Cs deposition was estimated at 0.6–0.8 (Terada et al., 2012). The total atmospheric deposition of ^{137}Cs after the accident was 100–300 kBq m⁻², based on the third airborne monitoring survey by the Japanese Government (MEXT, 2011). The mean annual air temperature and precipitation measured at the meteorological station located in Iitate village, 8.6 km southwest of our study site were 10.0 °C and 1361.6 mm, respectively (Japan

Meteorological Agency database from <http://www.jma.go.jp/jma/index.html>). The study site is a typical naturally regenerating forest (a secondary forest), which is dominated by deciduous broadleaf trees (e.g., Japanese oak, *Quercus crispula*) with sporadic evergreen coniferous trees (e.g., Japanese fir, *Abies firma*). The soil type at the study site is brown forest soil (Kanno et al., 2008).

A 20 × 20 m plot was established in the study site (tilted at less than 2° towards the northeast). No herbaceous plants were present in the study plot; only litter constituted ground cover. The thickness of the litter layer was approximately 2 cm and the layer was generally homogeneous with no bare areas. Ninety-one trees were present in the plot with a stand density of 2275 ha⁻¹ (only trees with a diameter at breast height (DBH) of ≥5 cm were counted). The largest tree in the plot was a Japanese fir (*Abies firma*) with a DBH of 46 cm. Sixteen species were recorded; Japanese oak (*Quercus crispula*) and Japanese fir (*Abies firma*) were dominant, accounting for 35% and 25% of total tree number, respectively. Other species were equal to or less than 5% of the total tree number. The crown projection diagram of the study plot given in Fig. 2a was drawn on July 28, 2015.

To compare the effects of canopy interception, wash-out with precipitation (throughfall, and stemflow) on soil radiocesium inventory and its spatial variation, we divided the study plot into five subplot types as shown in Fig. 2b: tree trunk base areas of evergreen coniferous trees (hereafter evergreen tree base areas, EB), tree trunk base areas of deciduous broadleaf trees (hereafter deciduous tree base areas, DB), areas under evergreen coniferous crowns excluding tree trunk base areas (hereafter, under evergreen crown areas, EC), areas under deciduous broadleaf crowns excluding tree trunk base areas (hereafter under deciduous crown areas, DC), and crown gap areas (CG). The EB and DB subplots in the present study included an area of less than 0.5 m radius from each tree, which was expected to be strongly affected by stemflow (Matsubayashi et al., 1994; Nakajima and Kaneko, 2012). The EC and DC subplots were determined according to the canopy projection diagram (Fig. 2a). To clarify effects of stemflow and throughfall separately, EC and DC did not include the areas around the tree trunk base. As shown in Fig. 2a, some areas of EB and EC were overlapped with those of DB and DC. In that case, these areas were considered as EB and EC because the canopy interception rates and translocation amounts of radiocesium with stemflow, throughfall and litterfall of evergreen coniferous trees were larger than those of

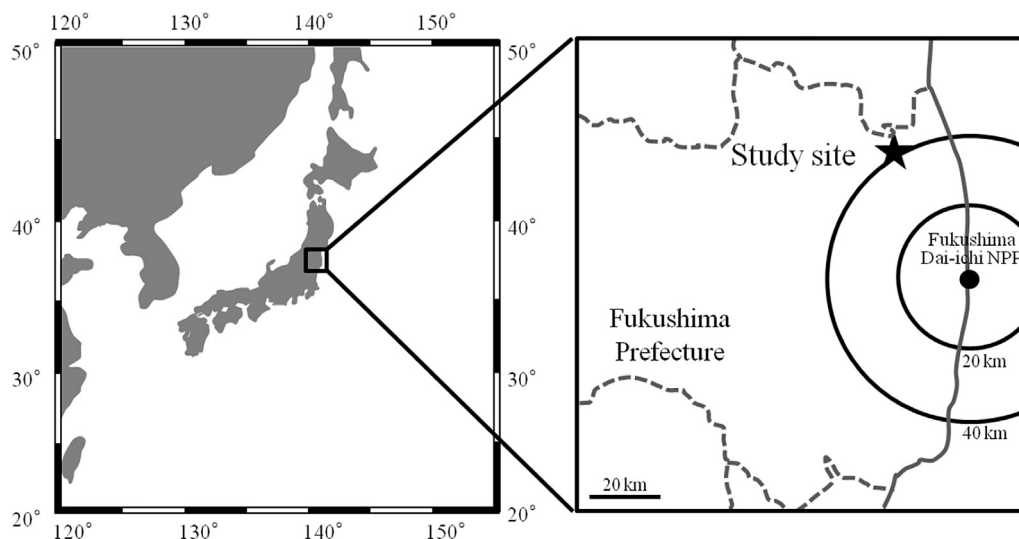


Fig. 1. Location of the study site and the Fukushima Daiichi Nuclear Power Plant.

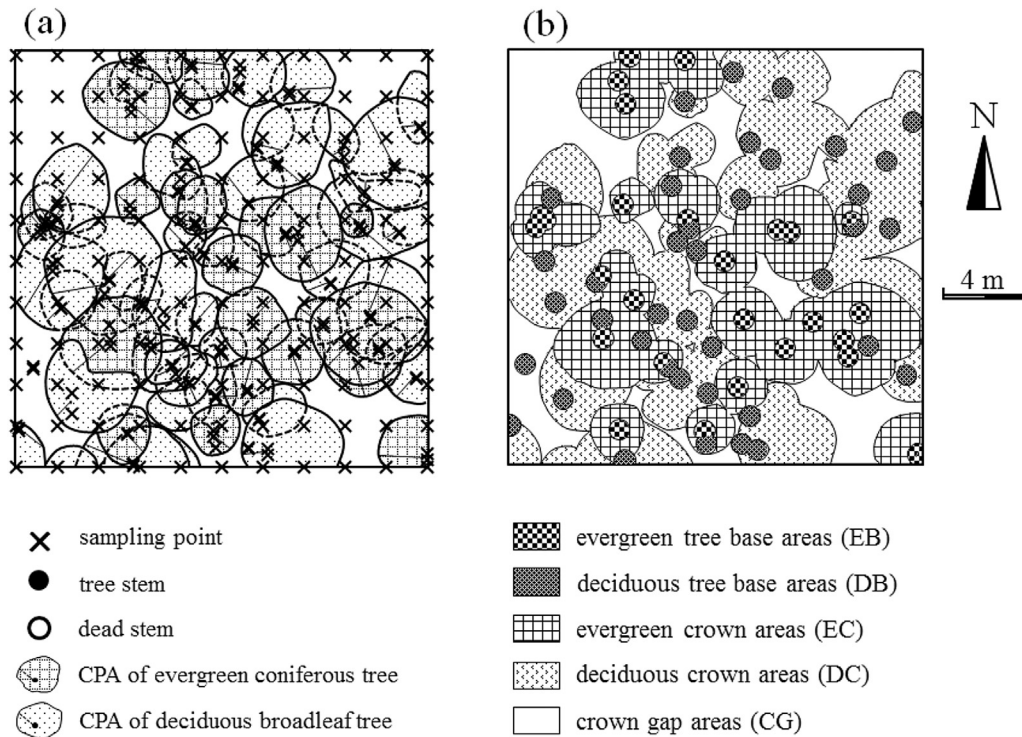


Fig. 2. Locations of soil sampling and crown projection diagram in the study plot (a), and the five subplot types for comparison of the soil ^{137}Cs inventory (b): evergreen tree base areas (EB), deciduous tree base areas (DB), areas under evergreen coniferous crowns excluding tree trunk base areas (EC), areas under deciduous broadleaf crowns excluding tree trunk base areas (DC), and crown gap areas (CG).

deciduous broadleaf trees (Kato et al., 2015; Endo et al., 2015). The CG was considered areas other than under trees including trees outside the plot, and the areas was 0.9–32 m². As the crown projection diagram at the time of the FDNPP accident is not expected to show large differences with this crown projection diagram, we used it for the analysis. The DBH growth of the trees in the present plot is estimated to be only a few centimeters and the consequent increase of the canopy projection areas is estimated to be very small after the accident (Hashizume, 1989; Shimano, 1997).

2.2. Collecting samples and radiocesium measurements

We decided to focus on the examination of spatial variation at the soil surface (0–5 cm soil depth excluding the litter layer) because we consider this layer to be more important than litter and deeper soil for the following reasons. Currently, most radiocesium within forest ecosystems in the Fukushima region is present within the upper 5 cm of soil (Takahashi et al., 2015). In addition, we found that the ^{137}Cs inventory at the soil surface (0–5 cm in depth) at the present study site accounted for more than 72% of that from litter layer to 10 cm of soil as on 31 July 2014 (Table 1). In addition, we have found that spatial variation of the ^{137}Cs inventory in the litter

layer was smaller than that in soil in mixed deciduous forests in Fukushima (Table 1; M. Takada, unpublished data). Finally, radiocesium in soil shows low mobility (Schimmack et al., 1994; Matsunaga et al., 2013), while the mobility in the litter layer is assumed to be relatively high because of the movement of litter around the forest floor under processes such as wind (Yamamoto and Bunzl, 1993). Accordingly, spatial variation of radiocesium in litter and soil should be examined separately.

We collected surface soil (0–5 cm depth) with a 100 mL-soil sampler (20 cm² and 5 cm depth) at 121 points in the 2-m grid plot on 31 July 2014 (Fig. 2a). In addition to the sample collection on the grids, we also collected soil samples in tree trunk base areas (EB and DB) of all identified trees in the plot from 129 points on 7 November 2014 (Fig. 2a). The soil samples were collected from the north- and south-facing sides of each tree within a distance of 10 cm from the tree trunk, and the radiocesium activities were measured separately. Some sampling points from the north and south sides of trees overlapped when trees were closely positioned. As some Japanese oak trees in the plot had been coppiced, soil samples from these coppices were collected from the north and south sides of the stocks.

The collected soil samples were dried at 100 °C for 48 h. The samples were filled into 100-mL plastic polypropylene containers (U-8) and analyzed for ^{137}Cs and ^{134}Cs using a low-background Ge spectrometer (GEM-110225, Seiko EG&G). The measurement times were between 600 and 10,000 s, depending on the radioactivity of the samples. The associated errors were composed of 5% from the detection efficiency and 1–5% from peak counting error. Activity of ^{137}Cs and ^{134}Cs in all samples showed a similar pattern, and the ratio of ^{137}Cs – ^{134}Cs activity was almost constant (1.0–1.1 in March 2011). In the present study, we only employed ^{137}Cs data for the determination of the spatial distribution of radionuclides. The ^{134}Cs data were not used because the relatively short half-life (2.06

Table 1
Depth distributions of ^{137}Cs inventory as on 31 July 2014.

	Litter layer	Soil (0–5 cm)	Soil (5–10 cm)
Geometric mean (kBq/m ²)	13	164	45
Range	5–22	43–376	20–230
CVg (CVa) ^a	0.47 (0.04)	0.50 (0.03)	1.03 (0.07)
n	8	8	8

^a CVg indicates ratio of the standard deviation of log-transformed ^{137}Cs inventory to the geometric mean. CVa indicates ratio of the standard deviation of ^{137}Cs inventory to the arithmetic mean.

Table 2
Descriptive statistics for soil ^{137}Cs inventory (kBq m^{-2}) in the entire study plot and the five subplot types.

	Geometric mean (kBq m^{-2}) ^a	Range	CVg (CVa) ^b	N	Area (m^2)
Total	202	22–697	0.11 (0.52)	250	400
Evergreen tree base areas (EB)	204 ^{ab}	22–624	0.12 (0.51)	57	18
Deciduous tree base areas (DB)	248 ^a	57–697	0.09 (0.47)	85	30
Evergreen crown areas (EC)	189 ^{ab}	57–439	0.11 (0.48)	27	117
Deciduous crown areas (DC)	170 ^b	24–574	0.11 (0.53)	49	147
Crown gap areas (CG)	156 ^b	56–438	0.09 (0.46)	32	89

^a Different letters indicate statistically significant differences between these areas (ANOVA test with multiple comparisons).

^b CVg indicates ratio of the standard deviation of log-transformed ^{137}Cs inventory to the geometric mean. CVa indicates ratio of the standard deviation of ^{137}Cs inventory to the arithmetic mean.

years) is unsuitable for this analysis more than three years after the FDNPP accident. Activity of ^{137}Cs was corrected for radioactive decay to the first sampling day of this survey: 31 July 2014. In the present study, we discussed the spatial variation of soil ^{137}Cs by inventory (Bq m^{-2}). The radiocesium activity of whole the soil samples collected with the 100 mL-soil sampler was measured and the inventory was calculated by dividing the ^{137}Cs activity by the area of the sampler (20 cm^2).

2.3. Statistical analysis

Application of the Shapiro–Wilk normality test showed that some datasets in the present study were logarithmically normal distributions ($P > 0.05$), although the remaining datasets were marginally not ($P < 0.05$). Many studies after the Chernobyl

accident showed that approximation of soil ^{137}Cs inventory with logarithmically normal distribution is suitable for statistical analysis (Khomutinin et al., 2004; Shcheglov et al., 2001). Therefore, all the datasets in the present study were log-transformed and a parametric test was used for statistical analysis.

Geometric means of the ^{137}Cs inventory (kBq m^{-2}), the coefficient of variation (ratio of the standard deviation of log-transformed ^{137}Cs inventory to the geometric mean, hereafter CVg), and the arithmetic coefficient of variation for comparisons with those in previous research (ratio of the standard deviation to the arithmetic mean, hereafter CVa) were calculated. The one-way analysis of variance (ANOVA) test with multiple comparisons (Tukey's test) was used to compare ^{137}Cs inventory between the five subplot types (EB, DB, EC, DC and CG).

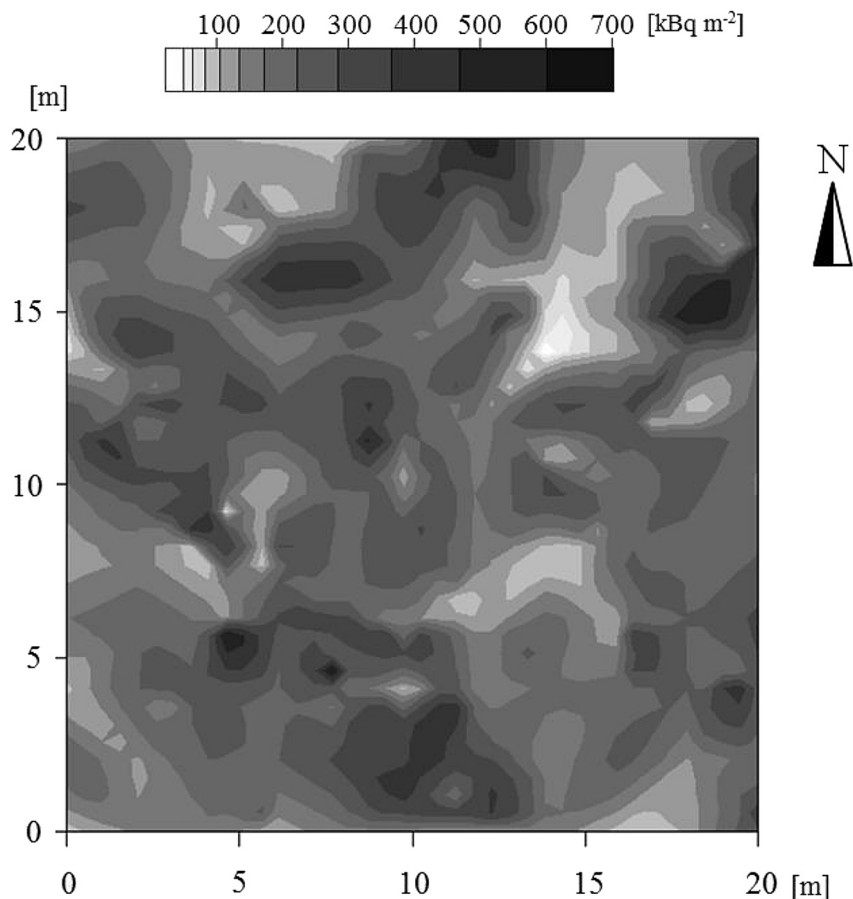


Fig. 3. Spatial distribution of soil ^{137}Cs inventory (kBq m^{-2}) in the study plot. Activity of ^{137}Cs was corrected for radioactive decay to the first sampling day of this survey: 31 July 2014.

3. Results

The geometric mean of the ^{137}Cs inventory in the study plot and the CVg were 202 kBq m^{-2} and 0.11 (0.52 in CVa), respectively. The range of the inventory was from 22 to 697 kBq m^{-2} , showing a difference of approximately 30 times and large spatial heterogeneity in the $20 \times 20 \text{ m}$ area (Table 2, Fig. 3). The ^{137}Cs inventory in the DB subplots showed the highest value (248 kBq m^{-2} in geometric mean) and lowest was in the CG areas (156 kBq m^{-2}). The CVg (CVa) values in the EB and DC subplots were relatively large at 0.12 (0.51) and 0.11 (0.53), respectively; however, the values for CG were small at 0.09 (0.46). The ^{137}Cs inventories showed statistically significant differences between the five subplot types (one-way ANOVA; $F_{4, 239} = 5.7, P < 0.001$). The ^{137}Cs inventory in the DB subplot was higher than those in the DC and CG subplots.

Fig. 4 shows frequency distributions of the ^{137}Cs inventories in the study plot and the five subplots. The magnitudes of all the histograms showed significant spreads in values and right-handed asymmetry (skewness, 0.4–1.3). In CG, over 56% of the inventory

was in the $100\text{--}200 \text{ kBq m}^{-2}$. In contrast, the frequent inventory varied in the under tree areas (EB, DB, EC and DC), and a higher number of the lowest and highest inventory samples ($0\text{--}100$ and $> 200 \text{ kBq m}^{-2}$) were observed under evergreen trees (EB and EC) than those under deciduous trees (DB and DC) and CG.

4. Discussion

The ^{137}Cs inventory in the present study plot showed large spatial heterogeneity and had a CVa value of 0.52. The CVa of Chernobyl-derived radiocesium inventory in a pine and oak forest soil was from 0.31 to 0.58, showing large spatial variation that is similar to our results (0–4 cm depth; Korobova and Romanov, 2009). These CVa values in forests were larger than those estimated for open areas (excluding forests) in Fukushima and the neighboring prefectures soon after the FDNPP accident (0.36 on average; Onda et al., 2015; Saito et al., 2015) collected soil samples in areas under homogeneous conditions (e.g. flat, no obstacles, no vegetation coverage).

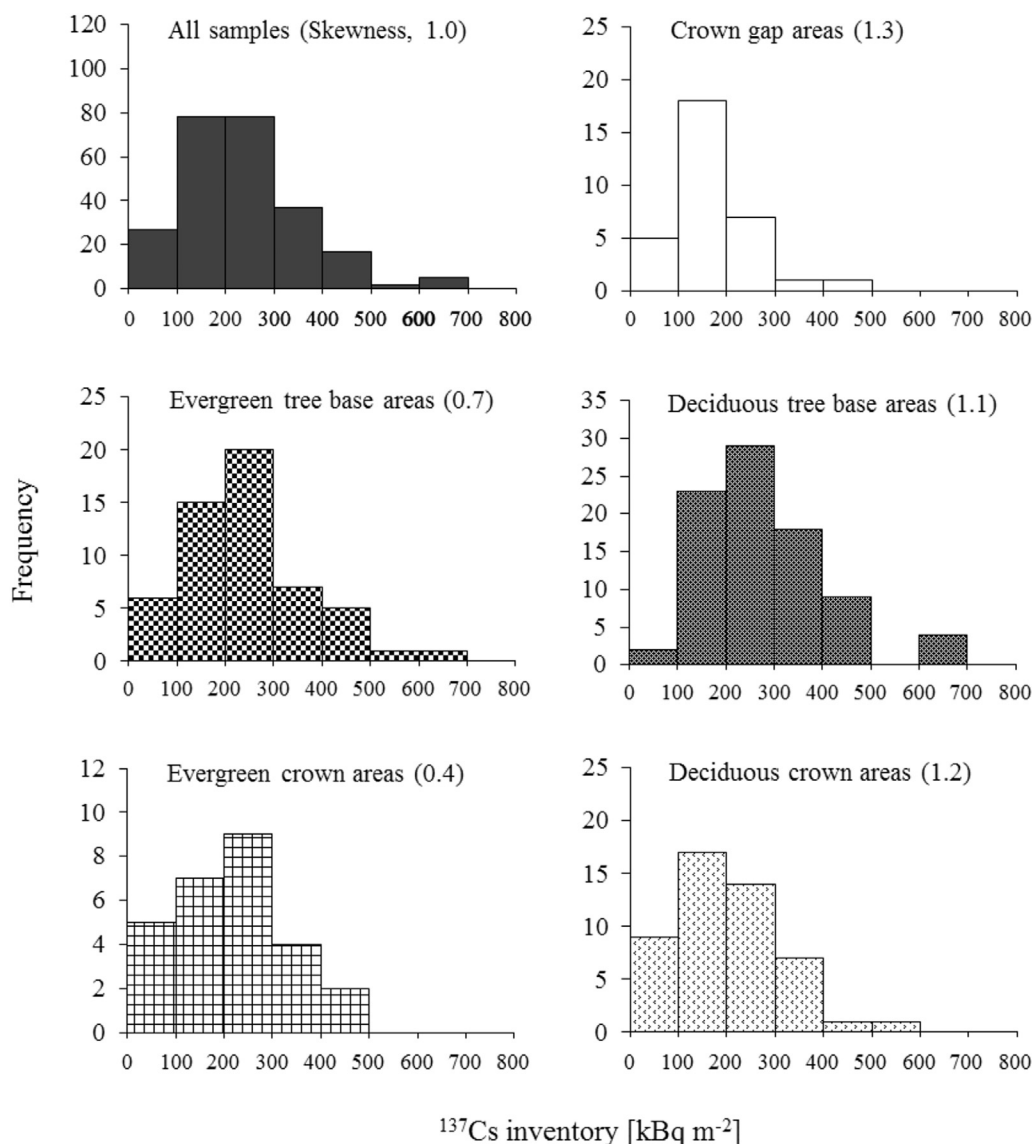


Fig. 4. Frequency distributions of soil ^{137}Cs inventory (kBq m^{-2}) and the skewness in the entire study plot and the five subplot types. The five subplot types correspond to those identified in Fig. 2b.

The large spatial heterogeneity in the present study plot is assumed to be strongly affected by initial transprocesses after the accident (from initial deposition to wash-out with precipitation). Even in the present study plot (20 × 20 m), the spatial variation differed among the five subplots; the spatial variation in the CG subplots was smaller than those under trees. The spatial variation in CG is thought to mainly reflect initial deposition and migration with litter decomposition. In other subplots that were located under trees (EB, DB, EC and DC), more samples of lower and higher inventory were observed. This result indicates that the presence of trees increases the spatial variation of soil radiocesium inventory (increases heterogeneity) as of three years after the FDNPP accident. This larger spatial variation in EB, DB, EC and DC may be due to several processes including canopy interception of initial deposition and wash-out of radiocesium on tree bodies with precipitation. Kato et al. (2015) reported that canopy interception was 70% and 20% of the total deposition in evergreen and deciduous forests, respectively, at the time of the accident in Fukushima Prefecture. The initial deposition under trees was also expected to be smaller than that in crown gap areas in our study site, leading to some soil samples with low radiocesium inventory. This also supports the finding that more of the lower inventory samples were observed under evergreen trees (EB and EC) than under deciduous trees (DB and DC). In addition, radiocesium intercepted by trees is transferred on and into forest floors and soils by precipitation through the processes of stemflow and throughfall (Endo et al., 2015; Kato et al., 2015). Accordingly, some high inventory samples may be observed where stemflow and throughfall were likely to have seeped.

The geometric mean of the inventory around tree areas was higher than that under tree crowns in some distance from the trees although the spatial variation under trees was very large. Yamamoto and Bunzl (1993) reported the similar spatial gradients in a German forest after the Chernobyl accident and attributed their findings to the process of radiocesium on trees washing out and seeping around tree trunk bases. The spatial gradients in the present study site differed between evergreen coniferous trees and deciduous broadleaf trees; the inventory gradually decreased from the tree trunk bases of evergreen coniferous trees although there were no statistically significant differences (EB ≥ EC ≥ CG). In contrast for the deciduous broadleaf trees, the inventory in DB was high and suddenly decreased under DC, showing almost the same inventory values to CG (DB > DC ≥ CG). A similar difference was observed by Yamamoto and Bunzl (1993) between beech trees (deciduous) and spruce trees (evergreen). This may be attributed to the phenological difference between evergreen and deciduous trees (only evergreen trees were in leaf at the time of the respective incidents).

5. Conclusion

Our result showed that the spatial variation of soil radiocesium inventory under trees (around tree trunk bases and under tree crowns) was larger than those in crown gap areas at our study site. The soils under the trees were thought to be strongly affected by some processes such as canopy interception and translocation by precipitation (throughfall and stemflow) soon after the accident, leading to areas of low and high radiocesium inventory values in the forest soil.

In the emergency soil sampling protocol, five soil samples within a 3 × 3 m area are recommended as the minimum number for reducing measurement uncertainty (Onda et al., 2015). Our result implies that more than five soil samples may be required in forest ecosystems to enhance the accurate evaluation of the radiocesium inventory.

Acknowledgments

We sincerely thank the landowners for permitting us to conduct the field survey. We also thank Prof. Y. Onda at the Center for Research in Isotopes and Environmental Dynamics, University of Tsukuba for the many useful suggestions, and Profs. K. Shizuma and S. Endo at the Graduate School of Engineering, Hiroshima University for their support for sample measurements. This study was supported by the Japan Society for the Promotion of Science KAKENHI Grant Number 15J03548, and the Hiroshima University Phoenix Leader Education Program (Hiroshima Initiative) for the “Renaissance from Radiation Disaster”, funded by the Ministry of Education, Culture, Sports, Science and Technology.

References

- Bunzl, K., Schimmack, W., Kreutzer, K., Schierl, R., 1989. Interception and retention of Chernobyl-derived ¹³⁴Cs, ¹³⁷Cs and ¹⁰⁶Ru in a spruce stand. *Sci. Total Environ.* 78, 77–87.
- Endo, I., Ohte, N., Iseda, K., Tanoi, K., Hirose, A., Kobayashi, N., Murakami, M., Tokuchi, N., Ohashi, M., 2015. Estimation of radioactive 137-cesium transportation by litterfall, stemflow and throughfall in the forests of Fukushima. *J. Environ. Radioact.* 149, 176–185.
- Endo, S., Kimura, S., Takatsuji, T., Nanasawa, K., Imanaka, T., Shizuma, K., 2012. Measurement of soil contamination by radionuclides due to the Fukushima Dai-ichi nuclear power plant accident and associated estimated cumulative external dose estimation. *J. Environ. Radioact.* 111, 18–27.
- Fujii, K., Ikeda, S., Akama, A., Komatsu, M., Takahashi, M., Kaneko, S., 2014. Vertical migration of radiocesium and clay mineral composition in five forest soils contaminated by the Fukushima nuclear accident. *Soil Sci. Plant Nutr.* 60, 751–764.
- Guillitte, O., Andolina, J., Koziol, M., Debauche, A., 1990. Plant-cover influence on the spatial distribution of radiocesium deposits in forest ecosystems. In: Desmet, G., Nassimbeni, P., Belli, M. (Eds.), *Transfer of Radionuclides in Natural and Semi-natural Environments*. Elsevier Applied Science, London, UK, pp. 441–449.
- Hashimoto, S., Matsuura, T., Nanko, K., Linkov, I., Shaw, G., Kaneko, S., 2013. Predicted spatio-temporal dynamics of radiocesium deposited onto forests following the Fukushima nuclear accident. *Sci. Rep.* 3, 2564.
- Hashizume, H., 1989. On the growth and timber price of some useful broad-leaved trees. *Hardwood Res.* 5, 13–20.
- Hisadome, K., Onda, Y., Kawamori, A., Kato, H., 2013. Migration of radiocesium with litterfall in hardwood-Japanese red pine mixed forest and Sugi plantation. *J. Jpn. For. Soc.* 95, 267–274.
- Kanno, H., Hirai, H., Takahashi, T., Nanzyo, M., 2008. Soil regions map of Japan based on a reclassification of the 1:1 million soil map of Japan (1990) according to the unified soil classification system of Japan: 2nd approximation (2002). *Pedologist* 52, 129–133.
- Katata, G., Ota, M., Terada, H., Chino, M., Nagai, H., 2012. Atmospheric discharge and dispersion of radionuclides during the Fukushima Dai-ichi nuclear power plant accident. Part I: source term estimation and local-scale atmospheric dispersion in early phase of the accident. *J. Environ. Radioact.* 109, 103–113.
- Kato, H., Onda, Y., Gomi, T., 2012. Interception of the Fukushima reactor accident-derived ¹³⁷Cs, ¹³⁴Cs and ¹³¹I by coniferous forest canopies. *Geophys. Res. Lett.* 39, L20403.
- Kato, H., Onda, Y., Hisadome, K., Loffredo, N., Kawamori, A., 2015. Temporal changes in radiocesium deposition in various forest stands following the Fukushima Dai-ichi nuclear power plant accident. *J. Environ. Radioact.* <http://dx.doi.org/10.1016/j.jenvrad.2015.04.016>.
- Khomutinin, Y.V., Kashparov, V.A., Zhebrovska, K.I., 2004. *Sampling Optimisation when Radioecological Monitoring*. Ukraine Institute for Agricultural Radiology, Kiev, Ukraine, ISBN 966-646-034-3.
- Korobova, E., Romanov, S., 2009. A Chernobyl ¹³⁷Cs contamination study as an example for the spatial structure of geochemical fields and modeling of the geochemical field structure. *Chemom. Intell. Lab. Syst.* 99, 1–8.
- Korobova, E., Romanov, S., 2011. Experience of mapping spatial structure of Cs-137 in natural landscape and patterns of its distribution in soil top sequence. *J. Geochem. Explor.* 109, 139–145.
- Kuroda, K., Kagawa, A., Tonosaki, M., 2013. Radiocesium concentrations in the bark, sapwood and hardwood of three species collected at Fukushima forests half a year after the Fukushima Dai-ichi nuclear accident. *J. Environ. Radioact.* 122, 37–42.
- Loffredo, N., Onda, Y., Kawamori, A., Kato, H., 2014. Modeling of leachable ¹³⁷Cs in throughfall and stemflow for Japanese forest canopies after Fukushima Daiichi nuclear power plant accident. *Sci. Total Environ.* 493, 701–707.
- Matsubayashi, U., Takagi, F., Velasquez, G.T., Sasuga, H., Sumi, T., 1994. On the effects of vegetation on infiltration and the flow path in mountainous slopes. *Proc. Hydraul. Eng.* 38, 185–190.
- Matsunaga, T., Koarashi, J., Andoh, A.M., Nagao, S., Sato, T., Nagai, H., 2013. Comparison of the vertical distributions of Fukushima nuclear accident radiocesium

- in soil before and after the first rainy season, with physicochemical and mineralogical interpretations. *Sci. Total Environ.* 447, 301–314.
- MEXT, 2011. Results of the Third Airborne Monitoring Survey by MEXT. <http://radioactivity.nsr.go.jp/en/list/307/list-1.html> (accessed 25.10.01).
- Nakajima, G., Kaneko, N., 2012. The effect of Japanese cypress plantation on soil biochemical characteristics converted from deciduous forests. *J. Jpn. For. Soc.* 94, 112–119.
- Onda, Y., Kato, H., Hoshi, M., Takahashi, Y., Nguyen, M.L., 2015. Soil sampling and analytical strategies for mapping fallout in nuclear emergencies based on the Fukushima Dai-ichi nuclear power plant accident. *J. Environ. Radioact.* 139, 300–307.
- Ono, K., Hiradate, S., Morita, S., Hirai, K., 2013. Fate of organic carbon during decomposition of different litter types in Japan. *Biogeochemistry* 11, 7–21.
- Rafferty, B., Dawson, D., Kliashtorin, A., 1997. Decomposition in two pine forests: the mobilisation of ^{137}Cs and K from forest litter. *Soil Biol. Biochem.* 29, 1673–1681.
- Rafferty, B., Brennan, M., Dawson, D., Dowding, D., 2000. Mechanisms of ^{137}Cs migration in coniferous forest soils. *J. Environ. Radioact.* 48, 131–143.
- Saito, K., Tanihata, I., Fujiwara, M., Saito, T., Shimoura, S., Otsuka, T., Onda, Y., Hoshi, M., Ikeuchi, Y., Takahashi, F., Kinouchi, N., Saegusa, J., Seki, A., Takemiya, H., Shibata, T., 2015. Detailed deposition density maps constructed by large-scale soil sampling for gamma-ray emitting radioactive nuclides from the Fukushima Dai-ichi nuclear power plant accident. *J. Environ. Radioact.* 139, 308–319.
- Schimmack, W., Bunzl, K., Dietl, F., Klotz, D., 1994. Infiltration of radionuclides with low mobility (^{137}Cs and ^{60}Co) into a forest soil: effect of the irrigation intensity. *J. Environ. Radioact.* 24, 53–63.
- Shcheglov, A.I., Tsvetnova, O.B., Klyashtorin, A.I., 2001. Biogeochemical Migration of Technogenic Radionuclides in Forest Ecosystems. Nauka, Moscow.
- Shimano, K., 1997. Analysis of relationship between DBH and crown projection area using a new model. *J. For. Res.* 2, 237–242.
- Takahashi, J., Tamura, K., Suda, T., Matsumura, R., Onda, Y., 2015. Vertical distribution and temporal changes of ^{137}Cs in soil profiles under various land uses after the Fukushima Dai-ichi nuclear power plant accident. *J. Environ. Radioact.* 139, 351–361.
- Terada, H., Katata, G., Chino, M., Nagi, H., 2012. Atmospheric discharge and dispersion of radionuclides during the Fukushima Dai-ichi nuclear power plant accident. Part II: verification of the source term and analysis of regional-scale atmospheric dispersion. *J. Environ. Radioact.* 112, 141–154.
- Yamamoto, M., Bunzl, K., 1993. Environmental effect studies on a forest ecosystem in Germany transport of chernobyl-derived radiocesium in a forest. *Radioisotopes* 42, 180–188.
- Yoshida, N., Kanda, J., 2012. Tracking the Fukushima radionuclides. *Science* 336, 1115–1116.